Novel CLCN5 mutations in patients with Dent's disease result in altered ion currents or impaired exchanger processing

Teddy Grand, David Mordasini, Sébastien L'Hoste, Thomas Pennaforte, Mathieu Genete, Marie-Jeanne Biyeyeme, Rosa Vargas-Poussou, Anne Blanchard, Jacques Teulon, Stéphane Lourdel

kidney INTERNATIONAL ISN

Novel *CLCN5* mutations in patients with Dent's disease result in altered currents or impaired processing

Journal:	*Kidney International*
Manuscript ID:	KI-12-08-1863.R2
Manuscript Type:	Original Article-Basic Research
Date Submitted by the Author:	
Complete List of Authors:	Grand, Teddy; UPMC Université Paris 06, UMR 7134; CNRS, UMR 7134 Mordasini, David; UPMC Université Paris 06, UMR 7134; CNRS, UMR 7134 L'Hoste, Sébastien; UPMC Université Paris 06, UMR 7134; CNRS, UMR 7134 Pennaforte, Thomas; UPMC Université Paris 06, UMR 7134; CNRS, UMR 7134 Genete, Mathieu; UPMC Université Paris 06, UMR 7134; CNRS, UMR 7134 Biyeyeme, Marie-Jeanne; UPMC Université Paris 06, UMR 7134; CNRS, UMR 7134 Vargas-Poussou, Rosa; Assistance Publique-Hôpitaux de Paris, Département de Génétique / HEGP; Université Paris-Descartes, Faculté de Médecine Blanchard, Anne; Assistance Publique-Hôpitaux de Paris, Département de Génétique / HEGP; Université Paris-Descartes, Faculté de Médecine Teulon, Jacques; UPMC Université Paris 06, UMR 7134; CNRS, UMR 7134 Lourdel, Stéphane; UPMC Université Paris 06, UMR 7134; CNRS, UMR 7134
Subject Area:	Transport
Keywords:	Cell & Transport Physiology, Dent-s disease, ion transport

scholarONE Manuscript Central

Novel *CLCN5* mutations in patients with Dent's disease result in altered currents or impaired processing

Teddy Grand[1,2], David Mordasini[1,2], Sébastien L'Hoste[1,2], Thomas Pennaforte[1,2], Mathieu Genete[1,2], Marie-Jeanne Biyeyeme[1,2], Rosa Vargas-Poussou[3,4], Anne Blanchard[5], Jacques Teulon[1,2] and Stéphane Lourdel[1,2].

[1]UPMC Université Paris 06, UMR 7134, F-75005, Paris, France; [2]CNRS, UMR 7134, F-75005, Paris, France; [3]Assistance Publique-Hôpitaux de Paris, Hôpital Européen George Pompidou, F-75908, Paris, France; [4]Université Paris-Descartes, Faculté de Médecine, F-75006, Paris, France; [5]Assistance Publique-Hôpitaux de Paris, Hôpital Européen Georges Pompidou, Centre d'Investigation Clinique, F-75908, Paris, France

Running head: ClC-5 mutations in Dent's disease

Word count: 3523

Address for correspondence:

Stéphane Lourdel, UMR 7134 CNRS/UPMC, 15 rue de l'Ecole de Médecine, 75720 Paris Cedex 06, France

phone: 33.1.55.42.78.55

fax: 33.1.46.33.41.72

e-mail: stephane.lourdel@upmc.fr

ABSTRACT

Dent's disease is an X-linked recessive disorder affecting the proximal tubules, and is frequently associated with mutations in *CLCN5*, which encodes the electrogenic Cl^-/H^+ exchanger ClC-5. Here, we screened five new *CLCN5* mutations, consisting of four missense mutations (G179D, S203L, G212A, L469P) and one nonsense mutation (R718X), and three published mutations (L200R, C219R and C221R). Their functional consequences were investigated in *Xenopus laevis* oocytes and HEK293 cells expressing either wild-type or mutant ClC-5. Two different types of mutant could be distinguished. The type-I mutant (G212A) trafficked normally to the cell surface and to early endosomes, like wild-type ClC-5, but exhibited significantly reduced currents. The type-I mutant underwent complex glycosylation at the cell surface, like wild-type ClC-5. Type-II mutants (G179D, L200R, S203L, C219R, C221R, L469P and R718X) were improperly N-glycosylated and were shown to be non-functional because of endoplasmic reticulum retention. In conclusion, we have identified distinct mechanisms by which mutations in *CLCN5* could impair ClC-5 function in Dent's disease.

KEYWORDS

Dent's disease; chloride/proton exchanger; ClC-5; mutation

INTRODUCTION

Dent's disease is a heterogeneous group of X-linked inherited disorders that have in common a renal phenotype consisting mainly of the urinary loss of low-molecular-weight protein (LMWP), hypercalciuria, nephrocalcinosis, and progressive renal failure, all of which are sometimes associated with other proximal tubule dysfunctions. Inactivating mutations of *CLCN5* are present in approximately two thirds of patients, whereas mutations of *OCRL1*, a gene encoding a Phospho-Inositide (PI) phosphatase, have been reported in only a few cases.[1,2]

CLCN5 encodes ClC-5, an electrogenic Cl^-/H^+ exchanger.[3,4] In the kidney, ClC-5 is predominantly expressed in the proximal tubule and α-intercalated cells of the collecting duct. Lower levels are also expressed in the thick ascending limb of Henle's loop.[5,6] In proximal tubule cells, ClC-5 is present on the membranes of intracellular subapical vesicles, where it colocalizes with the v-type H^+-ATPase, markers of early endosomes and proteins that have just been internalized by endocytosis.[5-9] This suggests that ClC-5 may neutralize currents of vesicular H^+-ATPases and that ClC-5 loss-of-function could lead to the defective endocytosis observed in the syndrome by impairing the crucial step of endosomal acidification.[6,10-12] ClC-5 disruption also led to a trafficking defect of megalin and its co-receptor cubilin.[10,13] Furthermore, ClC-5 may also contribute to protein-protein interactions required for receptor-mediated endocytosis at the proximal tubule cell surface as a result of its binding with cofilin,[14] an actin-depolymerizing protein, the PDZ-domain protein NHERF2,[15] and Nedd-4,[16] which by ubiquinating ClC-5 at its PY motif may shuttle it from the cell surface into early endosomes. Thus, as a whole, the mechanisms by which ClC-5 dysfunction results in Dent's disease still remain largely unknown.

Despite the large number of *CLCN5* mutations already reported, there has so far been only two reports providing a full functional analysis of some ClC-5 mutations.[17,18] Here, we report data that help to shed more light on the functional implications of ClC-5 in Dent's disease by describing five new and three previously reported *CLCN5* mutations, and investigating their consequences in *X. laevis* oocytes and HEK293 in terms of electrical activity, protein trafficking, expression and subcellular localization.

RESULTS

Clinical data from patients carrying the previously unreported mutations are shown in Table 1. All these patients presented with low-molecular-weight-proteinuria, hypercalciuria and/or nephrocalcinosis, and at least one other renal proximal tubular defect (glycosuria, aminoaciduria, phosphaturia).

To characterize the *CLCN5* mutations, we injected the corresponding human ClC-5 mutants and wild-type (WT) ClC-5 cRNA into oocytes. Two-electrode voltage-clamp recordings revealed strongly outwardly-rectifying currents from the oocytes expressing WT ClC-5, as previously reported (Figure 1A-B).[3,4,19,20] The currents for the G212A mutant were significantly reduced by 56% (n = 18) by comparison to oocytes expressing WT ClC-5 (Figure 1A). Despite reduced current amplitude, the voltage dependence of the currents for the G212A mutant resembled those of WT ClC-5 (Figure 1). In good agreement with a residual ClC-5 activity, currents from this mutant were reduced with partial replacement of extracellular Cl^- by I^-, an anion for which WT ClC-5 has lower permeability (data not shown).[19] In contrast, we failed to record any currents with the G179D (n = 26), S203L (n = 6), C219R (n = 22), L469P (n = 14), R718X (n = 13) mutants (Figure 1A). The L200R (n = 7) and C221R (n = 22) mutants were also found to be non-functional, as already reported.[18,21]

To further elucidate the mechanisms leading to reduced currents, we then investigated the cell surface targeting of WT and mutant ClC-5 proteins. The normalized chemiluminescence signals for the G212A mutant were not different from those of WT ClC-5, indicating that there was no impairment of cell surface expression with this mutant (Figure 2). These findings suggested that the significant decrease in current amplitudes for the G212A mutant (Figure 1A-B and Figure 2) were not due to impairment in protein trafficking to the cell surface. This could be explained by changes in conductance or in the regulation of the

mutant proteins. In contrast, the normalized chemiluminescence signals for the G179D, L200R, S203L, C219R, L469P and R718X mutants were not different from those observed in non-injected oocytes. No surface expression was detected with the C221R mutant, as had already been demonstrated.[18] The absence of significant electrical activity in oocytes carrying these mutants could be explained by an impairment of cell surface expression due to a mistargeting (Figure 1A-B, Figure 2) or by altered protein expression.

Total cell lysates isolated from oocytes expressing either WT or mutant ClC-5 were subjected to a western blot analysis (Figure 3A). In the lane loaded with WT ClC-5, a ~90-100 KDa diffuse immunoreactive band was detected, consistent with data already reported.[10] On the one hand, when an equivalent amount of proteins was loaded in each lane, no significant difference in density or size could be detected between WT ClC-5 and the G212A mutant. Thus, the decreased currents of the G212A mutant were not attributable to different protein expression levels. On the other hand, expression of the G179D, L200R, S203L, C219R, and L469P mutants was reduced compared to WT ClC-5. This could be explained by a change in the processing of the mutant proteins. The C221R mutant also showed this reduced protein expression, which conflicted with previously published data.[18] The R718X mutant exhibited a band smaller than those of WT ClC-5, as would be expected for the truncation mutation, and the protein abundance was lower than that of WT ClC-5.

The diffuse immunoreactive band observed with WT ClC-5 at ~90-100 kDa suggested that hClC-5 may have undergone post-translational modification, as previously described.[22] To gain more insight into the processing of WT and mutant forms of ClC-5, total cell lysates were treated with the Endo H and PNGase F (Figure 3B and C). Endo H cleaves high-mannose glycosylations, and some hybrid oligosaccharides form of N-linked glycoproteins. Therefore, Endo H-sensitive proteins likely remain in the endoplasmic reticulum without further processing, and are only core-glycosylated. PNGase F cleaves complex, hybrid, and

high-mannose glycosylations. The lane loaded with WT ClC-5 demonstrated specific bands of ~90 and ~100 kDa. The 90 kDa band of WT ClC-5 was sensitive to Endo H, whereas the 100 kDa band was not (Figure 3B). This indicates that the 90 kDa protein contains high-mannose glycosylation and is retained in the endoplasmic reticulum, whereas the 100 kDa protein contains complex glycosylation. In contrast, the 100 kDa band was sensitive to PNGase F (Figure 3B). The Endo H and PNGase F digestion showed that the core protein migrated with an apparent molecular size of 83 kDa (Figure 3B). Similar treatments revealed that the G212A mutant displayed the WT ClC-5 complex glycosylation (Figure 3C). In contrast, only core-glycosylation was observed with the C219R mutant (Figure 3C). The G179D, L200R, S203L, C221R, L469P and R718X mutants also exhibited core-glycosylation (data not shown).

Thus, abolition of conduction and surface expression for the G179D, L200R, S203L, C219R, C221R, L469P and R718X mutants are compatible with impaired N-glycosylation, which is likely to result in rapid degradation of the products within the cell.

To further document the subcellular localization of WT and mutants ClC-5, we performed confocal microscopy imaging of indirect immunofluorescence in transiently transfected HEK293 cells. As shown in Figure 4, WT ClC-5 staining colocalized with biotinylated cell-surface proteins and with the early endosomes marker EEA1. A weak colocalization between WT ClC-5 and the endoplasmic reticulum marker calnexin was also observed. Likewise, the G212A mutant colocalized with biotinylated cell-surface proteins and EEA1. To further confirm plasma membrane expression for WT ClC-5 and the G212A mutant, we carried out surface biotinylation experiments. No significant difference could be detected in the surface fraction containing WT ClC-5 compared with the G212A mutant (Figure 5). Interestingly, in contrast to the total cell lysates, the biotinylated protein fraction contained only the complex-type glycosylated fraction of ClC-5, indicating that the plasma membrane ClC-5 component is complex glycosylated. In contrast, the G179D, L200R,

S203L, C219R, C221R, L469P and R718X mutants were retained in the endoplasmic reticulum compartment, as shown by their colocalization with the endoplasmic reticulum marker calnexin, and were excluded from the plasma membrane and the early endosomes (Figure 4). Surface biotinylation experiments also demonstrated that the C219R mutant was excluded from the surface biotinylated protein fraction (Figure 5). The G179D, L200R, S203L, L469P and R718X mutants were also excluded from the apical biotinylated protein fraction (data not shown). As a whole, abolition of conduction and surface expression of these mutants are compatible with their endoplasmic reticulum retention, which is likely to result in rapid degradation of the products within the cell.

DISCUSSION

Here, we have explored the functional effects of five novel *CLCN5* mutations found in patients with Dent's disease, including four missense mutations (G179D, S203L, G212A and L469P) and one nonsense mutation (R718X), plus three previously published missense mutations (L200R, C219R and C221R).

The G179D, L200R, S203L, C219R, C221R, L469P and R718X mutants displayed a defective protein surface expression, electrical activity and lacked the complex glycosylation showed by WT ClC-5. Our immunocytochemical analysis in HEK293 transfected cells revealed that these mutants are not detected at the cell surface because they are retained in the endoplasmic reticulum, probably due to improper folding. As a consequence, they may be subjected to early degradation by quality control mechanisms thus accounting for their reduced protein expression and their core-glycosylation form. As far as we are aware, only one *CLCN5* mutation is known to result in impaired N-glycosylation, the G333R mutation located in the J helix.[23] The authors speculated that the mutation may induce a disruption of the interface between the homodimers,[24,25] and that would lead in turn to the formation of misfolded proteins and rapid degradation. These data do not help to explain our findings, because the five missense mutations are located quite some distance from the transporter interface. However, it is interesting to note that apart from G179D and R718X they are all located in α-helices (Figure 6). These mutations may significantly affect the stability of the α-helices, thus enhancing protein degradation. Lack of complex glycosylation is usually observed in mutant proteins not reaching the plasma membrane. This is the case for instance for the NCC protein carrying mutations for Gitelman syndrome.[26,27] However, Schmieder *et al.* studying *X. laevis* ClC-5 (xClC-5) with mutations on N-glycosylation sites observed that a

significant fraction of non-glycosylated xClC-5 mutants escaped from endoplasmic reticulum retention and was targeted to the plasma membrane.[28]

Our results for the R718X mutant, which predict a loss of 28 amino acids from the C-terminus and a deletion of a part of CBS2 domain, are in sharp contrast with previous findings reported for the Y617X, R648X and R704X ClC-5 mutants that affect the CBS1 and CBS2 domains. Residual activity was found for the R648X mutant,[18] but not for the Y617X and R704X mutants.[21,29] However, the last three mutants were all found to be targeted to the cell surface, with an increase in surface expression for the R648X mutant.[18,30,31] Our findings raise the possibility that the R718X mutation may interfere with the proper folding of the C-terminus of ClC-5 that is necessary to pass the quality controls of the endoplasmic reticulum.

In contrast to the previous mutants, the G212A mutant underwent further processing and appeared to be modified into complex glycosylated forms, and trafficked to the cell surface and to the early endosomes, like WT ClC-5.

This mutant displayed reduced currents with normal cell surface expression. The G212A mutation is located at the beginning of helix F (Figure 5).[24,25] It directly follows the "gating glutamate" which is responsible for coupling the Cl^- flux to the H^+ counter-transport in ClC Cl^-/H^+ exchangers.[3,4,32] Neutralization of the "gating glutamate" converted EcClC-1, ClC-4 and ClC-5 into pure anion conductances and abolished the strong outward rectification of ClC-4 and ClC-5.[3,4,32] Here, we demonstrated that the G212A mutation reduced the electrical activity without abolishing the outward rectification. Several mechanisms can account for the reduced currents amplitudes: the mutation could eliminate the H^+ coupling to Cl^-, the mutant protein could exhibit lower transport rates, the stoichiometry of Cl^-/H^+ coupling could be modified and the probability of the mutant protein of being in an active state could be affected. Future studies are needed to examine the specific effects of the G212A mutation.

By using whole-cell recordings and a vesicular acidification assay in HEK-MSR cells expressing ClC-5 pathogenic mutations, Smith *et al.* recently demonstrated that the R280P mutation resulted in altered electrical activity, reduced plasma membrane expression, increased expression in early endosomes and enhanced endosomal acidification. To explain the abnormal decrease of intraluminal pH, the authors raised the hypothesis that an accumulation of the mutant protein in early endosomes would ideally support and enhance endosomal acidification.[17] Here, we have demonstrated that the G212A mutant also displayed reduced electrical activity like the R280P mutant. However, because the G212A mutant trafficked normally to the plasma membrane and early endosomes like WT ClC-5, further investigations are required to determine the possible effects of the mutation on the intraluminal pH.

In conclusion, two types of ClC-5 mutants can be distinguished. Type-I mutants are properly targeted to the plasma membrane and early endosomes, but with reduced electrical activity (G212A). Type-I mutants are complex glycosylated. Type-II mutants fail to induce currents, because of defective processing in N-glycosylation resulting of endoplasmic reticulum retention (G179D, L200R, S203L, C219R, C221R, L469P and R718X).

MATERIALS AND METHODS

DNA Sequence analysis of the *CLCN5* gene

Peripheral blood samples were obtained and genomic DNA was extracted by standard methods. The coding exons (2 to 12) and intron-exon junctions were amplified with *CLCN5*-specific primers described elsewhere using PCR amplification.[33] We carried out direct sequencing using the dioxy chain termination method on an automated Perkin Elmer/Applied Biosystems Division 373A Stretch DNA capillary sequencer, and evaluated sequences with Sequencher software.

Molecular Biology

ClC-5 mutants were synthesized from human wild-type ClC-5 extracellularly HA tagged and subcloned either into the pTLN expression vector for expression in *X. laevis* oocytes or into the peGFP expression vector for expression in HEK293 cells. The coding sequence for GFP in the peGFP vector have been substituted for those of WT or mutant ClC-5. Site directed mutagenesis was performed with the Quickchange site-directed mutagenesis kit (Stratagene, La Jolla, CA, USA). All constructs were fully sequenced.

Expression in *X. laevis* oocytes

Capped cRNA were synthetized *in vitro* from wild-type and mutants ClC-5 expression vectors using the SP6 mMessage mMachine Kit (Ambion, Austin, TX, USA). Defolliculated *X. leavis* oocytes were injected with 20 ng of the different cRNAs and were then kept at 17°C in modified Barth's solution containing (in mM): 88 NaCl, 1 KCl, 0.41 $CaCl_2$, 0.32 $Ca(NO_3)_2$, 0.82 $MgSO_4$, 10 HEPES, pH 7.4 and gentamicin (20 µg/ml).

Electrophysiology

Five days after injection, two-electrode voltage-clamp experiments were performed at room temperature using a TEV-200A amplifier (Dagan, Minneapolis, MN, USA) and PClamp 8 software (Axon Instruments, USA). Currents were recorded in ND96 solution containing (in mM): 96 NaCl, 2 KCl, 1.5 $CaCl_2$, 1 $MgCl_2$, 5 HEPES, pH 7.4. For pH 5.5 and 6.5, 5 mM HEPES was replaced by 5 mM MES. In the iodide substitution experiment, 80 mM Cl^- was replaced by equivalent amounts of I^-. Currents were recorded in response to a voltage protocol consisting of 20 mV steps from –100 mV to +100 mV during 800 ms from a holding potential of –30 mV.

Surface labeling of oocytes

Experiments were essentially performed as previously described,[34] using a rat monoclonal anti-HA antibody (3F10, Roche Diagnostics, Meyland, France) as primary antibody and a peroxidase-conjugated goat anti-rat antibody (Jackson ImmunoResearch, West Grove, PA, USA) as secondary antibody. Chemiluminescence was quantified in a Turner TD-20/20 luminometer (Turner Designs, Sunnyvale, CA, USA) by placing individual oocytes in 50 µl of SuperSignal Elisa Femto Maximum Sensitivity Substrate Solution (Pierce, Rockford, IL, USA).

Cell culture and transfection

HEK293 cells were grown in Dulbecco's modified Eagle's medium (DMEM) (GIBCO, invitrogen, CA, USA) supplemented with 10% fetal bovine serum, penicillin (100 units/ml), and streptomycin (100 µg/ml) at 37°C in 5% CO_2. The cells were transiently

transfected using Fugene 6 according to the manufacturer's instructions (Roche Diagnostics, Meyland, France).

Immunocytochemistry

Transfected HEK293 cells were plated on 12 mm diameter Petri dishes. Cells were then fixed in 4% paraformaldehyde and permeabilized with 0.3% Triton. Nonspecific binding sites were blocked with 16% goat serum solution. Primary antibodies were mouse anti-HA (Sigma, St Louis, MO, USA), rabbit anti-EEA1 (Sigma, St Quentin Fallavier, France), rabbit anti-calnexin (Stressgen, Ann Arbor, MI, USA). FITC-conjugated goat anti-mouse (Jackson ImmunoResearch, West Grove, PA, USA), TRITC-conjugated goat anti-rabbit (Jackson ImmunoResearch, West Grove, PA, USA), or Cy5-conjugated streptavidin (Sigma, St Quentin Fallavier, France) were added to the cells as secondary antibodies. Labeled cells were analyzed with a Zeiss LSM 510 confocal laser scanning microscope.

Surface biotinylation of HEK293 cells

48 h after transfection, cells were placed on ice and rinsed twice with a cold rinsing solution containing PBS, 100 µM $CaCl_2$ and 1 mM $MgCl_2$. Cells were then incubated at 4°C for 1 h with PBS and 1.5 mg/ml NHS-biotin (Pierce, Rockford, IL, USA). They were incubated in quenching solution containing 0.1% BSA diluted in PBS and rinsed 3 times with the rinsing solution. After lysis in a solution containing 20 mM Tris HCl, 2 mM EDTA, 2 mM EGTA, 30 mM NaF, 30 mM NaPPi, 1% Triton, 0.1% SDS and a protease inhibitor mix (Complete, Roche Diagnostics, France), equal amount of proteins were precipitated at 4°C overnight using streptavidin-agarose beads (Pierce, Rockford, IL, USA). Samples were then centrifuged at 2,500 x g during 2 min at 4°C with TLB solution containing 50 mM Tris-HCl, pH 7.4, 100 mM NaCl, 5 mM EDTA and the protease inhibitor mix.

Protein isolation

Total cell lysates were isolated from oocytes after homogenization of the cells in an ice-cold solution containing (in mM): 250 sucrose, 0,5 EDTA, 5 Tris-HCl, pH 7.4, and a protease inhibitor mix (Complete, Roche Diagnostics, France). Samples were centrifuged 3 times at 500 x g for 2 minutes to remove yolk platelets. Protein concentration in the resulting supernatant was quantified using a protein assay quantification kit (BCA Protein Kit Assay, Pierce, Rockfort, IL, USA). Digestion of proteins with N-glycosidase F (PNGase F) and endoglycosidase H (Endo H) (New England Biolabs, Ipswich, MA, USA) was performed according to the protocol provided by the manufacturer.

For the isolation of total cell lysates from HEK293, cells were incubated 10 min on ice with the lysis solution. Samples were centrifugated at 13,000 rpm for 5 minutes. Protein concentration in the supernatant was quantified using the protein assay quantification kit.

Western blot analysis

The proteins were separated on an 8% SDS-PAGE gel and transferred to PVDF membranes. Primary rat anti-HA monoclonal antibody (3F10, Roche Diagnostics, Meyland, France), rabbit anti-GAPDH monoclonal antibody (Abcam, Cambridge, UK) and secondary peroxidase-conjugated goat anti-rat antibody (Jackson ImmunoResearch, West Grove, PA, USA) and anti-rabbit (Promega, Madison, WI, USA) were diluted in TBS-blocking solution. Detection was performed using the ECL Western Blotting Substrate (Pierce, Rockford, IL, USA).

Statistics

Results are shown as mean ± SEM. *n* indicates the number of experiments. Significance was analyzed by a paired Student's t-test. $P < 0.05$ was considered significant.

DISCLOSURE

All the authors declare no competing interests.

REFERENCES

1. Ludwig M, Utsch B, Monnens LA. Recent advances in understanding the clinical and genetic heterogeneity of Dent's disease. *Nephrol Dial Transplant* 2006; **21**: 2708-2717.

2. Hoopes RR, Jr., Shrimpton AE, Knohl SJ, Hueber P, *et al.* Dent Disease with mutations in OCRL1. *Am J Hum Genet* 2005; **76**: 260-267.

3. Picollo A, Pusch M. Chloride/proton antiporter activity of mammalian CLC proteins ClC-4 and ClC-5. *Nature* 2005; **436**: 420-423.

4. Scheel O, Zdebik AA, Lourdel S, Jentsch TJ. Voltage-dependent electrogenic chloride/proton exchange by endosomal CLC proteins. *Nature* 2005; **436**: 424-427.

5. Devuyst O, Christie PT, Courtoy PJ, Beauwens R, *et al.* Intra-renal and subcellular distribution of the human chloride channel, CLC-5, reveals a pathophysiological basis for Dent's disease. *Hum Mol Genet* 1999; **8**: 247-257.

6. Gunther W, Luchow A, Cluzeaud F, Vandewalle A, *et al.* ClC-5, the chloride channel mutated in Dent's disease, colocalizes with the proton pump in endocytotically active kidney cells. *Proc Natl Acad Sci U S A* 1998; **95**: 8075-8080.

7. Dowland LK, Luyckx VA, Enck AH, Leclercq B, *et al.* Molecular cloning and characterization of an intracellular chloride channel in the proximal tubule cell line, LLC-PK1. *J Biol Chem* 2000; **275**: 37765-37773.

8. Sakamoto H, Sado Y, Naito I, Kwon TH, *et al.* Cellular and subcellular immunolocalization of ClC-5 channel in mouse kidney: colocalization with H^+-ATPase. *Am J Physiol* 1999; **277**: F957-965.

9. Suzuki T, Rai T, Hayama A, Sohara E, *et al.* Intracellular localization of ClC chloride channels and their ability to form hetero-oligomers. *J Cell Physiol* 2006; **206**: 792-798.

10. Piwon N, Gunther W, Schwake M, Bosl MR, *et al.* ClC-5 Cl^- channel disruption impairs endocytosis in a mouse model for Dent's disease. *Nature* 2000; **408**: 369-373.

11. Hara-Chikuma M, Wang Y, Guggino SE, Guggino WB, *et al.* Impaired acidification in early endosomes of ClC-5 deficient proximal tubule. *Biochem Biophys Res Commun* 2005; **329**: 941-946.

12. Gunther W, Piwon N, Jentsch TJ. The ClC-5 chloride channel knock-out mouse - an animal model for Dent's disease. *Pflugers Arch* 2003; **445**: 456-462.

13. Christensen EI, Devuyst O, Dom G, Nielsen R, *et al.* Loss of chloride channel ClC-5 impairs endocytosis by defective trafficking of megalin and cubilin in kidney proximal tubules. *Proc Natl Acad Sci U S A* 2003; **100**: 8472-8477.

14. Hryciw DH, Wang Y, Devuyst O, Pollock CA, *et al.* Cofilin interacts with ClC-5 and regulates albumin uptake in proximal tubule cell lines. *J Biol Chem* 2003; **278**: 40169-40176.

15. Hryciw DH, Ekberg J, Ferguson C, Lee A, *et al.* Regulation of albumin endocytosis by PSD95/Dlg/ZO-1 (PDZ) scaffolds. Interaction of Na^+-H^+ exchange regulatory factor-2 with ClC-5. *J Biol Chem* 2006; **281**: 16068-16077.

16. Hryciw DH, Ekberg J, Lee A, Lensink IL, *et al.* Nedd4-2 functionally interacts with ClC-5: involvement in constitutive albumin endocytosis in proximal tubule cells. *J Biol Chem* 2004; **279**: 54996-55007.

17. Smith AJ, Reed AA, Loh NY, Thakker RV, *et al.* Characterization of Dent's disease mutations of CLC-5 reveals a correlation between functional and cell biological consequences and protein structure. *Am J Physiol Renal Physiol* 2009; **296**: F390-397.

18. Ludwig M, Doroszewicz J, Seyberth HW, Bokenkamp A, *et al.* Functional evaluation of Dent's disease-causing mutations: implications for ClC-5 channel trafficking and internalization. *Hum Genet* 2005; **117**: 228-237.

19. Steinmeyer K, Schwappach B, Bens M, Vandewalle A, *et al.* Cloning and functional expression of rat CLC-5, a chloride channel related to kidney disease. *J Biol Chem* 1995; **270**: 31172-31177.

20. Friedrich T, Breiderhoff T, Jentsch TJ. Mutational analysis demonstrates that ClC-4 and ClC-5 directly mediate plasma membrane currents. *J Biol Chem* 1999; **274**: 896-902.

21. Lloyd SE, Pearce SH, Fisher SE, Steinmeyer K, *et al.* A common molecular basis for three inherited kidney stone diseases. *Nature* 1996; **379**: 445-449.

22. Jouret F, Igarashi T, Gofflot F, Wilson PD, *et al.* Comparative ontogeny, processing, and segmental distribution of the renal chloride channel, ClC-5. *Kidney Int* 2004; **65**: 198-208.

23. Tanuma A, Sato H, Takeda T, Hosojima M, *et al.* Functional characterization of a novel missense CLCN5 mutation causing alterations in proximal tubular endocytic machinery in Dent's disease. *Nephron Physiol* 2007; **107**: p87-97.

24. Dutzler R, Campbell EB, Cadene M, Chait BT, *et al.* X-ray structure of a ClC chloride channel at 3.0 A reveals the molecular basis of anion selectivity. *Nature* 2002; **415**: 287-294.

25. Wu F, Roche P, Christie PT, Loh NY, *et al.* Modeling study of human renal chloride channel (hCLC-5) mutations suggests a structural-functional relationship. *Kidney Int* 2003; **63**: 1426-1432.

26. Kunchaparty S, Palcso M, Berkman J, Velazquez H, *et al.* Defective processing and expression of thiazide-sensitive Na-Cl cotransporter as a cause of Gitelman's syndrome. *Am J Physiol* 1999; **277**: F643-649.

27. de Jong JC, Willems PH, van den Heuvel LP, Knoers NV, *et al.* Functional expression of the human thiazide-sensitive NaCl cotransporter in Madin-Darby canine kidney cells. *J Am Soc Nephrol* 2003; **14**: 2428-2435.

28. Schmieder S, Bogliolo S, Ehrenfeld J. N-glycosylation of the Xenopus laevis ClC-5 protein plays a role in cell surface expression, affecting transport activity at the plasma membrane. *J Cell Physiol* 2007; **210**: 479-488.

29. Yamamoto K, Cox JP, Friedrich T, Christie PT, *et al.* Characterization of renal chloride channel (CLCN5) mutations in Dent's disease. *J Am Soc Nephrol* 2000; **11**: 1460-1468.

30. Mo L, Xiong W, Qian T, Sun H, *et al.* Coexpression of complementary fragments of ClC-5 and restoration of chloride channel function in a Dent's disease mutation. *Am J Physiol Cell Physiol* 2004; **286**: C79-89.

31. Wang Y, Cai H, Cebotaru L, Hryciw DH, *et al.* ClC-5: role in endocytosis in the proximal tubule. *Am J Physiol Renal Physiol* 2005; **289**: F850-862.

32. Accardi A, Miller C. Secondary active transport mediated by a prokaryotic homologue of ClC Cl- channels. *Nature* 2004; **427**: 803-807.

33. Lloyd SE, Pearce SH, Gunther W, Kawaguchi H, *et al.* Idiopathic low molecular weight proteinuria associated with hypercalciuric nephrocalcinosis in Japanese children is due to mutations of the renal chloride channel (CLCN5). *J Clin Invest* 1997; **99**: 967-974.

34. Zerangue N, Schwappach B, Jan YN, Jan LY. A new ER trafficking signal regulates the subunit stoichiometry of plasma membrane K(ATP) channels. *Neuron* 1999; **22**: 537-548.

FIGURE LEGENDS

Figure 1. Electrophysiological properties of WT and mutants ClC-5. A. Steady-state current-voltage relationships obtained in ND96 solution (pH 7.4). Each data point represents the mean ± SEM for at least 6 oocytes from three different oocyte batches. *NI*, Non-Injected oocytes. **B.** Representative original voltage-clamp recordings obtained from oocytes expressing WT CLC-5, G179D mutant CLC-5, and from non-injected oocytes under same conditions as described in A.

Figure 2. Currents/cell surface expression relationship for WT and mutants ClC-5. Currents at +100 mV are from the same data as in Figure 1A. For cell surface expression, the values (measured in RLU, Relative Light Units) were normalized to those of WT ClC-5 in the same batch of oocytes. Each column represents the mean ± SEM for at least 6 oocytes for current recordings, and at least 60 oocytes from three different batches of oocytes for the surface expression. *, $P < 0.001$ is the difference between WT or mutants ClC-5 vs NI. #, $P < 0.001$ is the difference between NI or mutants ClC-5 vs WT ClC-5.

Figure 3. Western blot analysis of WT and mutants ClC-5. A. Total cell lysates were isolated from NI and injected oocytes. **B and C.** Total cell lysates were isolated from oocytes injected with WT or mutants ClC-5. Some preparations were treated with PGNase F (*F*) and Endo H (*H*). *CTL,* Control. Data are typical results for 40 oocytes from three different batches of oocytes.

Figure 4. Immunocytochemical localization of WT and mutants ClC-5 in HEK293 transfected cells. ClC-5 expression was detected by green fluorescence. Organelles were

stained with one of three markers : biotin (plasma membrane), EEA1 (early endosomes), calnexin (endoplasmic reticulum) and were detected by red fluorescence. The yellow fluorescence indicates that both proteins overlap. Scale bars, 7 µm.

Figure 5. Cell surface expression of WT and mutants ClC-5 in HEK293 transfected cells. **A.** Western blot analysis of the surface biotinylated protein fraction (S) or total cell lysates (T). **B.** Relative quantification of cell surface expression of WT and mutants ClC-5. Densitometric analysis of total and cell surface ClC-5 is shown as the ratio of biotinylated surface proteins to total cells lysates quantified by densitometry. Each column represents the mean ± SEM from 5 experiments. *UT*, untransfected cells.

Figure 6. Amino acid sequence alignment of several ClCs showing the position of the *CLCN5* mutations characterized in this study. The conserved regions are shown in bold and highlighted in gray. Mutations are shown above the sequences. The alignment was performed using BioEdit.

Table 1. Clinical and biochemical abnormalities in probands with Dent syndrome and new *CLCN5* mutations

	Patient 1	*Patient 2*	*Patient 3*	*Patient 4*	*Patient 5*	*Patient 6*
Age at first symptom (years)	4	8	7	3	4	1
Failure to thrive	+	-	-	-	-	-
LMWP	+	+	+	+	+	+
Hypercalciuria	+	-	+	+	+	+
Renal impairment	+[1]	-	-	-	-	+
Nephrocalcinosis	+	-	+	+ *	+	+
Nephrolithiasis	-	-	-	-	-	-
Phosphate diabetes	+	+	NA	-	-	-
Rickets	+	-	-	-	-	-
Aminoaciduria	+	-	NA	NA	-	+
Glycosuria	NA	NA	NA	-	-	-
Hypouricemia	NA	NA	NA	NA	+	+
Polyuria	+	-	-	-	-	-
Country	Portugal	Portugal	Belgium	North Africa	France	France
Mutation Nucleotide	c.1406T>C		c.635G>A	c.2152c>T	c.536G>A	c.608C>T
Protein	p.Leu469Pro		p.Gly212Ala	p.Arg718X	p.Gly179Asp	p.Ser203Leu

+ = present, - = absent. NA: not available. LMWP: low-molecular-weight-proteinuria. [1]Renal function impairment at 10 years.
* Nephrocalcinosis at 12 years. Numbering is according to the cDNA sequence (GenBank entry NM 000084). The A of the ATG of the initiator Methionine codon is denoted as nucleotide 1. Patients 1 and 2 are brothers.

ACKNOWLEDGMENTS

We thank Pr. T.J. Jentsch for kindly providing us the HA-tagged ClC-5, Pr. C. Korbmacher for helpful discussion about surface expression assay, G. Planelles for support and help with oocytes, the patients involved, and the clinicians who referred the patients for genetic studies: M.-P. Lavocat, V. Regemorter, R. Novo, C. Loirat and P. Cochat. We also thank Christophe Klein for excellent technical assistance in confocal microscopy. The English text was edited by M. Ghosh.

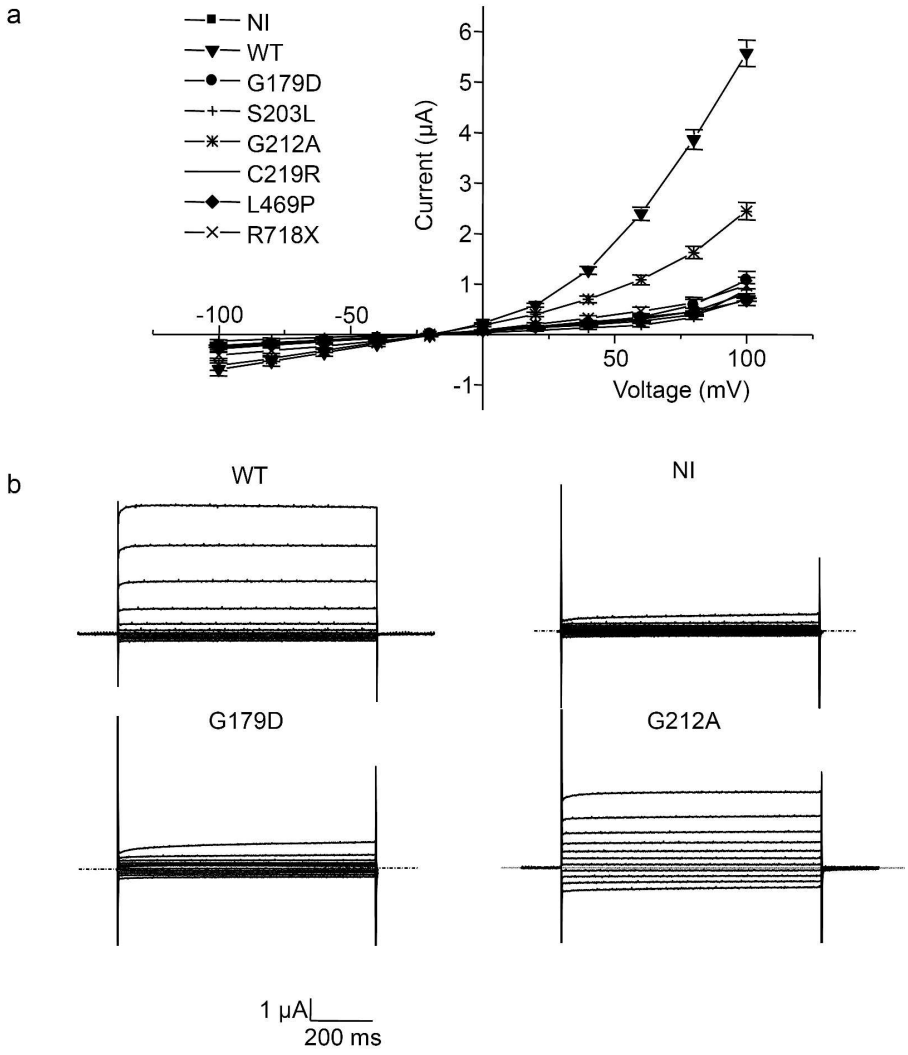

Figure 1

138x182mm (600 x 600 DPI)

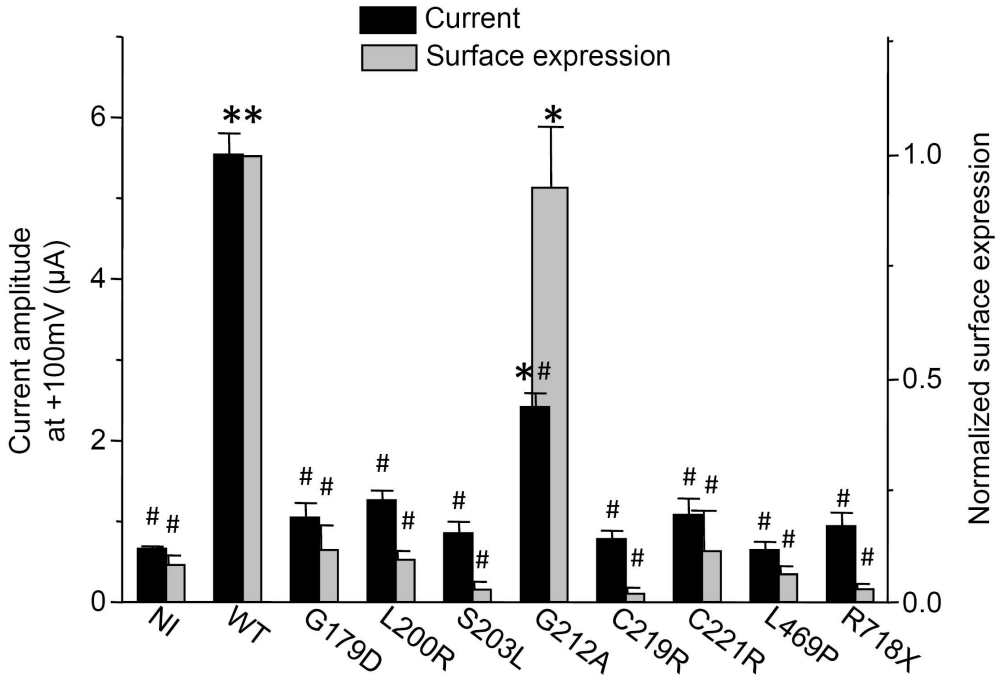

Figure 2

94x77mm (600 x 600 DPI)

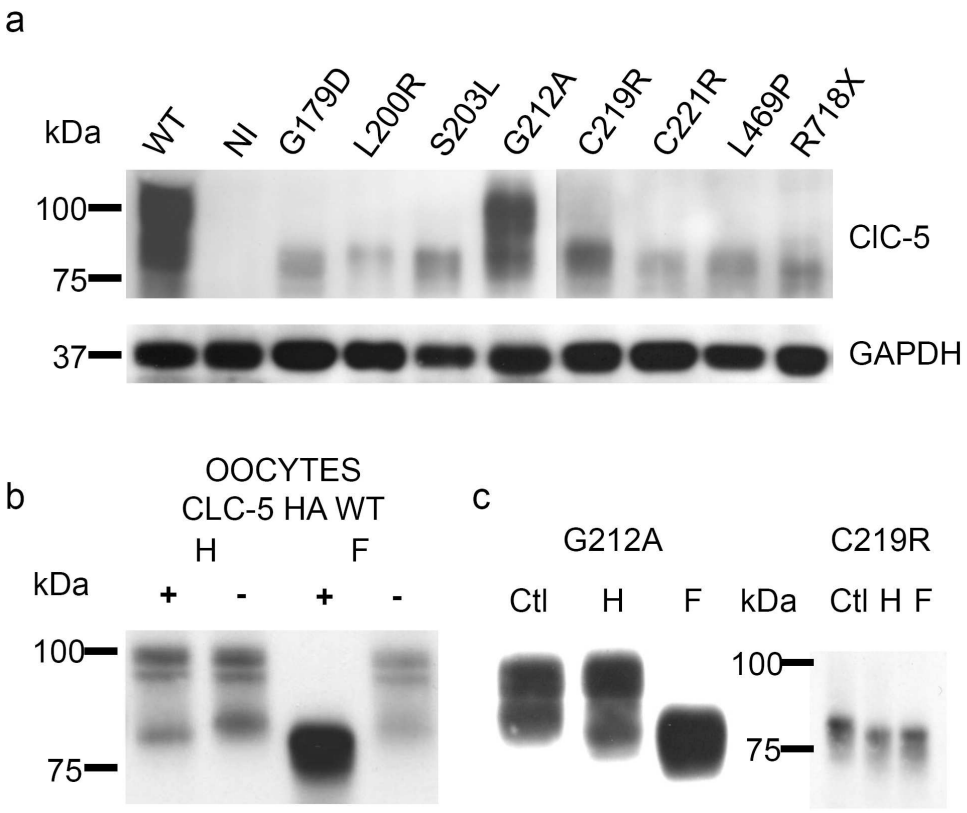

Figure 3

84x85mm (600 x 600 DPI)

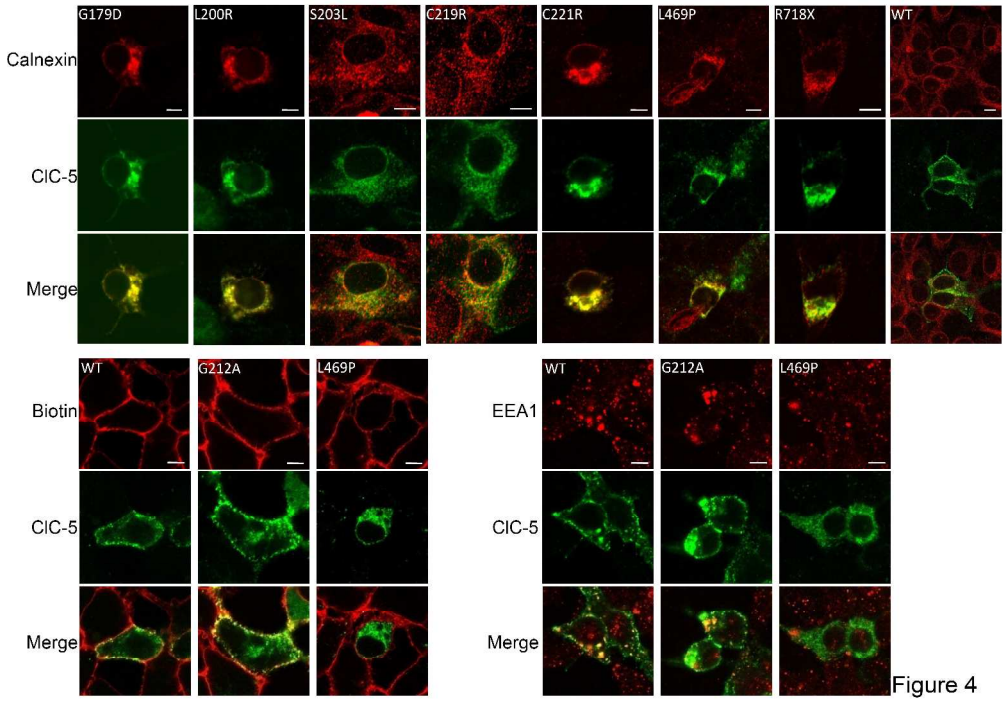

Figure 4

198x139mm (600 x 600 DPI)

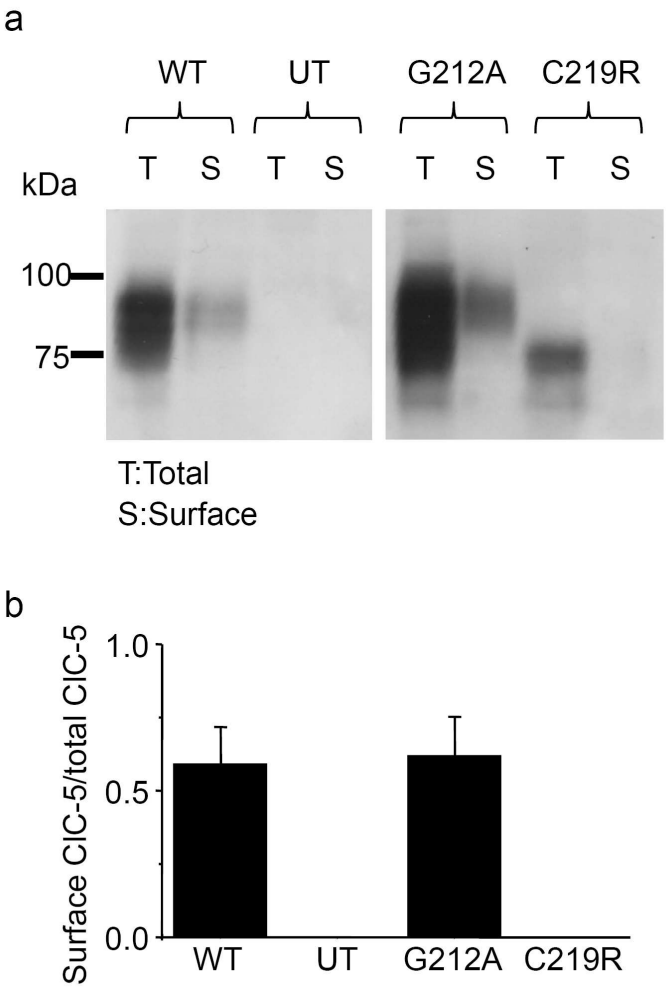

Figure 5

59x101mm (600 x 600 DPI)

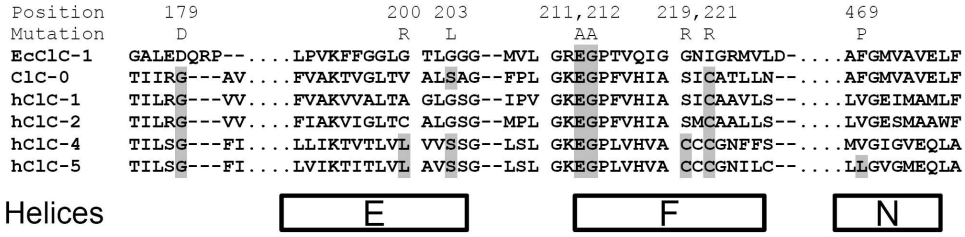

Figure 6

88x33mm (600 x 600 DPI)